

Cite this: DOI: 10.1039/c0xx00000x

www.rsc.org/xxxxxx

## ARTICLE TYPE

## Layered Double Hydroxide (LDH)-based Monolith with Interconnected Hierarchical Channels: Enhanced Sorption Affinity for Anionic Species

Yasuaki Tokudome,<sup>\*a</sup> Naoki Tarutani,<sup>a</sup> Kazuki Nakanishi<sup>b</sup> and Masahide Takahashi<sup>a</sup>*Received (in XXX, XXX) Xth XXXXXXXXX 20XX, Accepted Xth XXXXXXXXX 20XX*

DOI: 10.1039/b000000x

Monolithic layered double hydroxides (LDHs) with interconnected channels have been expected to enhance sorption rate as well as increase accumulation of anions. Although powder molding can form easy-handled LDH compacts, interconnected channel formation therein has not been achieved. Herein, we demonstrate cm-scale monolithic LDH-based composites with interconnected hierarchical channels via a spontaneous sol–gel reaction. The synthesis was performed on Mg–Al hydrotalcite-type LDHs starting from metal chlorides aqueous/ethanolic solution with poly(ethylene oxide) incorporated. Addition of propylene oxide triggers sol–gel reaction to form monolithic xerogels with a formula of  $[\text{Mg}_{0.66}\text{Al}_{0.33}(\text{OH})_2\text{Cl}_{0.33} \cdot 2.92\text{H}_2\text{O}] \cdot 3.1\text{Al}(\text{OH})_3$ . LDH crystals together with aluminum hydroxide crystals homogeneously build up gel skeletons with well-defined hierarchical channels. The interconnected channels in  $\mu\text{m}$  range (macrochannel) are formed as a phase-separated structure, whereas the channels in nm range (nanochannel) are as interstices of primary particles. The channel architectures are preserved in the course of rehydration process, affording enhanced sorption affinity for anion species in the process. Both of macro and mesochannels as well as high charge density of the obtained LDHs ( $\text{Mg}/\text{Al}=2.0$ ) contribute enhanced anion sorption in the monolithic xerogels. The materials obtained here opens up applications of high performance adsorbent and ion-storage free from diffusion limitation.

## Introduction

Oxide- and hydroxide-based crystals with a layered structure have drawn considerable attention due to their unique properties taking advantage in fields such as adsorption<sup>1, 2</sup>, separation<sup>3</sup>, catalysis<sup>4</sup>, and solar cells<sup>5</sup>. The anisotropy of two dimensional (2D) architecture has been demonstrated to serve as an ideal 2D quantum system for studying fundamental physics as well as a basic building block in the synthesis of functional solids.<sup>6</sup> The oxide- or hydroxide layers can be electrically-charged so that the oppositely-charged ions are introduced into interlayers. Controlled entrapping/releasing ions has been exploited for applications including drug delivery<sup>7</sup> and sensing applications<sup>8</sup>. The anisotropy of the confined interlayer space allows restricted 2D migration of ions, finding applications in the fields of storage and ion conductors<sup>9, 10</sup>. Hydrotalcite-like compounds are layered double hydroxides (LDHs) with the general formula of  $[\text{M}(\text{II})_{1-x}\text{M}(\text{III})_x(\text{OH})_2]^{x+}[\text{A}^{n-}_{x/n}]^{x-} \cdot z\text{H}_2\text{O}$ , where  $\text{A}^{n-}$  is charge compensating anion, M(II) and M(III) are di- and trivalent cations, respectively. The layered structure is composed of alternative stacking of positively charged hydroxide layers and intercalated charge compensating anions. Since a wide variety of cation species are incorporated in the hydroxide layer, a family of hydrotalcite-like compounds has been investigated as one of the promising layered crystals in the various aforementioned application fields.<sup>11–13</sup>

LDHs are typically synthesized as powdery crystals via co-precipitation<sup>14, 15</sup> in which cases subsequent powder molding processes is required for desired shapes in specific applications. For example in environmental purification, the use of monolithically-shaped LDHs would afford easy-handling and simplify the overall procedures by skipping a time-consuming separation/collection process of powdery ones. In spite of the potential advantages, monolithic LDHs which inherit considerable capabilities of ion-exchange and sorption have not been demonstrated. A drawback of the powder molding process is that intercalation paths, *i.e.*, layers' edges, and sorption sites on crystal surface are partly spoiled by additives for the shaping such as powder binders and modifiers.<sup>16, 17</sup> "diffusion limitation" is much more critical; diffusion of anions into a deep inside of monoliths takes a significant time, which in turns accessible ion-trapping sites are limited to a vicinity of the outer surface of the compacts.<sup>18, 19</sup> A promising way to improve anion diffusion is to fabricate diffusion channels inside monoliths. Sacrificial polymer templating has been a promising way for a formation of meso- and macropores in various materials.<sup>20–22</sup> However, this strategy generally results in isolated or weakly-interconnected pores when robust monolithic materials are attempted. It still remains challenging to fabricate monolithic LDHs with well-defined channels penetrating from outer surface to inner part.

With the purpose of breaking-through the limitations of existing materials, this study focuses on the fabrication of LDH-

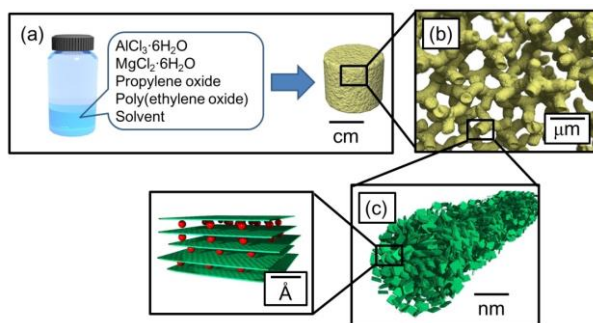


**Figure 1.** Schematic illustration of LDH-based monoliths with accessible hierarchical channels. (a) monolithic xerogels were prepared from metal salts and propylene oxide. (b) macrochannels are formed as a result of phase separation. (c) mesochannels are formed as interstices of primary/secondary particles.

based monoliths which have highly accessible hierarchical channels (Fig. 1). The LDH-based monoliths are synthesized via a sol-gel reaction from metal salts, propylene oxide (PO: proton scavenger), and poly(ethylene oxide) (PEO: phase separation initiator) (Fig. 1a). The incorporation of PO is crucial for a monolith formation without cracks by inducing a modest growth of pH. The formation of  $\mu\text{m}$ -sized channel (macrochannel) is performed by a technique based on phase separation parallel with sol-gel transition.<sup>23</sup> Co-continuous phase-separated domains solidified by sol-gel reaction forms interconnected macrochannel after removing a phase-separated fluid phase (Fig. 1b). Whereas the nm-sized channel (mesochannel) is spontaneously formed as interstices between primary particles (Fig. 1c). It should be highlighted that the strategy used in this study can be applicable to various types of LDHs owing to the simple reaction from metal salt precursors. The typical example presented herein is Al-Mg type LDH monoliths with interconnected channels. Starting compositions which afford spontaneous interconnected-channel formation as well as LDH crystallization have been demonstrated as Al-rich compositions ( $\text{Mg}/\text{Al} \leq 0.8$ ). The discussion in this study is mainly focused on a nominal molar ratio of  $\text{Mg}/\text{Al} = 0.8$ . The xerogels obtained here show distinguished structural features: (1) monolith with desired shapes and dimensions; (2) hierarchical interconnected channels; (3) nanocrystalline LDH of high anion-sorption capacity. The interconnected macrochannel and the high sorption capacity of LDH crystals significantly contribute to the improved diffusion and accumulation of anions. As a result, we have achieved enhanced accumulation of anionic species as well as drastically-improved sorption rate in monolithic LDHs with a cm-scale. The monolithic feature allows easy-handling and molding in a special container. The materials obtained here opens up applications of high performance adsorbent and ion-storage free from diffusion limitation.

## Experimental Section

### Preparation of LDH-based Monolithic Xerogels.

Aluminum chloride hexahydrate ( $\text{AlCl}_3 \cdot 6\text{H}_2\text{O}$ ; 98%) and magnesium chloride hexahydrate ( $\text{MgCl}_2 \cdot 6\text{H}_2\text{O}$ ; 98%) were used as an aluminum and a magnesium sources, respectively. A mixture of ultrapure water and ethanol ( $\text{EtOH}$ ; 99.5%) was used as a solvent. Poly(ethylene oxide) (PEO;  $M_v = 1 \times 10^6$ ) was used as a phase separation inducer. ( $\pm$ )-propylene oxide (PO;  $\geq 99\%$ ) was added as a proton scavenger to initiate gelation. Isopropyl alcohol (IPA; 99.7%) was used to exchange the solvent contained in wet gels. PEO and PO were purchased from Sigma-Aldrich Co.

and all other reagents were from Wako Pure Chemicals Industries, Ltd. All chemicals were used as received. Typical sample synthesis (a nominal molar ratio of  $\text{Mg}/\text{Al} = 0.80$ ) was performed as follows;  $\text{AlCl}_3 \cdot 6\text{H}_2\text{O}$  (1.58 g; 6.55 mmol),  $\text{MgCl}_2 \cdot 6\text{H}_2\text{O}$  (1.06 g; 5.23 mmol), and PEO (30.0 mg;  $3.00 \times 10^{-5}$  mmol) were dissolved in a mixture of water (4.00 mL; 222 mmol) and ethanol (3.00 mL; 51.4 mmol). At 25 °C, PO (1.82 mL; 26.2 mmol) was added to this solution and stirred for 1 min to form a homogenous sol. The sol was transferred into a polystyrene container, sealed, and kept at 40 °C to form a monolithic wet gel. The wet gel was aged for 24 h at 40 °C, subjected to solvent exchange with IPA. Subsequent evaporative drying at 40 °C produces a monolithic xerogel with a typical dimension of 1 cm  $\times$  1 cm  $\times$  3 mm. The preparation free from PEO additive was also examined according to the above procedure. For comparison, powdery hydrotalcite-type LDH intercalated by chloride ions was prepared according to the method reported by Constantino et al.<sup>14</sup> The powdery LDH was shaped into a pellet and used as a reference (See Supplementary Method S1). Some of the samples were calcined at 500 °C for 1 h. We hereafter denote the calcined xerogel and the calcined reference pellet as the c-gel and the c-pellet, respectively. Especially, we refer c-gel with only mesochannel as c-gel-meso and the c-gel with hierarchical channel as c-gel-hierarchical.

### Processing of rehydration with $\text{Na}_2\text{CO}_3$ .

Rehydration of a sample was investigated using  $\text{Na}_2\text{CO}_3$  aqueous solution, where  $\text{CO}_3^{2-}$  anions were used as a FTIR-detectable probe to double-check the recovery of the layered structure. The c-gel with macrochannel was immersed in 0.1 M  $\text{Na}_2\text{CO}_3$  aqueous solution for 24 h. The sample was separated from the solution and immersed in abundant ultra-pure water for washing. After a prescribed time period, water was decanted, and the monolith was dried at 40 °C.

### Processing of rehydration with Pyranine.

Rehydration processing with aqueous pyranine (trisodium 8-hydroxypyrene-1,3,6-trisulfonate; the structural formula is shown in the inset in Fig. 6(a)) solution was examined on c-gels and c-pellet. The samples have been cut to show a comparable external surface area of  $1.9 \times 10^2 \text{ mm}^2$ . Each sample was immersed in 10 mL of aqueous pyranine solution ( $19.1 \text{ mmol} \cdot \text{L}^{-1}$ ). 10  $\mu\text{L}$  of the supernatant was collected after various time periods, diluted 200 times with 1 M NaOH solution, analyzed by ultraviolet-visible spectroscopy (UV-Vis: V-670 spectrophotometer, JASCO Corp.). The concentration of pyranine in the solution was estimated by the Beer-Lambert law using peak intensity around at 455 nm.

### Characterization of xerogels.

Macro- and mesomorphologies of the samples were observed by a field emission scanning electron microscope (FE-SEM; S-4800, Hitachi, Japan, with a thin Au Pt/Pd coating) equipped with an energy-dispersive X-ray spectrometer (EDS). A transmission electron microscope (TEM; JEM-2000FX, JEOL, Japan) was employed at operating voltage of 200 kV to observe microstructures of the xerogel. For TEM observation, the monolithic xerogel was ground into fine powders and then dispersed in ethanol to form a slightly turbid suspension. A small drop of the resultant suspension was placed on a carbon-coated copper mesh grid and dried at room temperature. Crystal phases

**Table 1.** Crystal phase and morphology of xerogels prepared with various Mg/Al nominal molar ratios. The amounts of chemicals other than metal chlorides were set at an identical value which is described in experimental section.

		Mg/Al			
		0.5	0.8	3.0	5.0
Crystal Phase	LDH LDH + Mg(OH) <sub>2</sub>				
Morphology	Interconnected Channels Particle Aggregates				

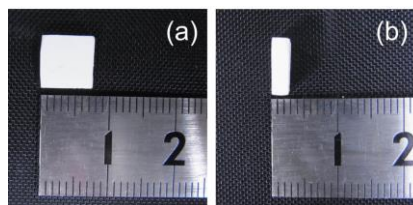


**Figure 2.** Representative photographs of LDH-based monolithic xerogel: (a) top view image; (b) side view image.

of the obtained samples were identified by X-ray diffraction (XRD; MultiFlex, Rigaku, Japan) using CuK $\alpha$  radiation ( $\lambda$  = 0.154 nm). Thermogravimetric–differential thermal analysis (TG–DTA; Thermo Plus Evo, Rigaku, Japan) was carried out at a ramp rate of 10 °C/min while continuously supplying air at a rate of 300 mL/min. Micro–mesoporous characters of the calcined samples (c-gels and c-pellet) were investigated by N<sub>2</sub> adsorption–desorption apparatus (BELSORP-mini II, Bel Japan Inc., Japan). Prior to the measurement, the sample was outgassed under vacuum at 100 °C. The pore size distribution was calculated from the adsorption branch of the isotherm by the Barrett–Joyner–Halenda (BJH) method, and the specific surface area was estimated by the Brunauer–Emmett–Teller (BET) method.

## Results and Discussion

### Fabrication of LDH-based monolithic xerogel

Mg<sup>2+</sup> and Al<sup>3+</sup> were adopted as di- and trivalent cations in [M(II)<sub>1-x</sub>M(III)<sub>x</sub>(OH)<sub>2</sub>]<sup>x+</sup>[A<sup>n−x/n</sup>]<sup>x−</sup>·zH<sub>2</sub>O. The metal salts in the starting solution was 4-times concentrated compared to typical starting compositions for powdery LDHs<sup>14</sup> so that gel networks develop to form a monolithic gel. The ethanol/water mixed solvent was used to prepare compatible starting mixtures, which affords homogeneous and monolithic gels. Upon addition of PO, pH in the solution rapidly increases from 1.0 to 2.0 in 1 min, and moderately reaches to 3.8 at 24 min (Supplementary Fig. S1). Gelation occurs in 18 min and subsequent drying process forms a monolithic xerogel. It has been reported that PO works as a proton scavenger through (1) protonation of epoxide oxygen and (2) a subsequent irreversible ring-opening reaction by nucleophilic anionic conjugate bases, such as Cl<sup>−</sup> and NO<sub>3</sub><sup>−</sup>.<sup>24</sup> In the present case, Cl<sup>−</sup> anions added as AlCl<sub>3</sub>·6H<sub>2</sub>O and MgCl<sub>2</sub>·6H<sub>2</sub>O works as nucleophilic anions to drive the reaction and increase pH in the solution. Although possible nucleophiles in this system are Cl<sup>−</sup> and H<sub>2</sub>O which competitively reacts with PO, Cl<sup>−</sup> anions are known to show much better nucleophilic

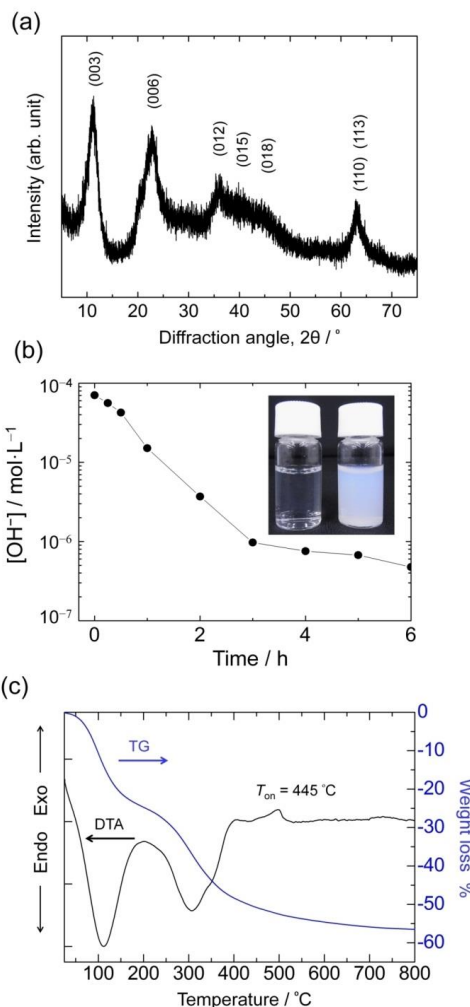


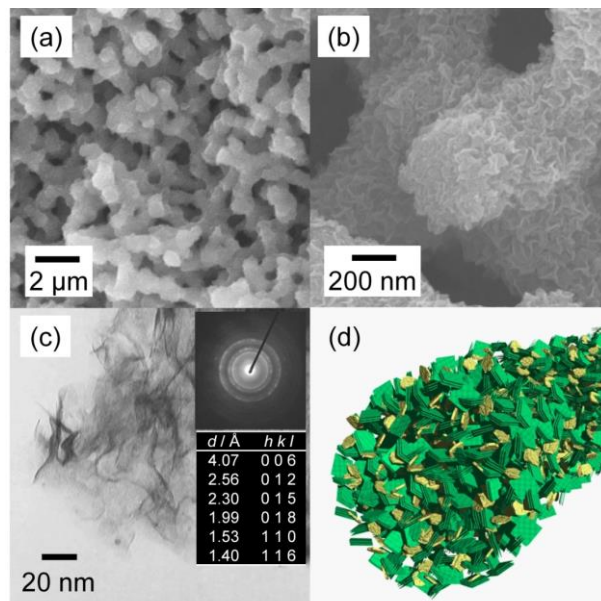
**Figure 3.** (a) XRD pattern of the LDH-based xerogel. (b) [OH<sup>−</sup>] vs time since the xerogel immersion in a NaOH solution (pH=10) at a weight ratio of xerogel/NaOH = 0.01. Time evolution of pH was recorded at room temperature. The inset images show the supernatant after reacting with xerogel for 12 h; (left) before and (right) after adding a AgNO<sub>3</sub> aqueous solution. (c) TG (blue) and DTA (black) curves of the LDH-based xerogel.  $T_{on}$ : onset temperature of crystallization.

characteristics against PO. Taking into account that the reaction between H<sub>2</sub>O and PO regenerate protons and does not increase pH in the solution,<sup>24, 25</sup> we have selected highly-concentrated metal chlorides solution as starting sols. It should be emphasized that the formation of homogeneous and monolithic gels requires the PO-mediated reaction under acidic conditions which have not been commonly used for LDH synthesis. Table 1 summarizes crystalline phase and morphology of materials prepared using various Mg/Al nominal ratios (0.5 ≤ Mg/Al ≤ 5.0). LDH forms at all the compositions we investigated, whereas interconnected channels forms with the starting compositions of 0.5 ≤ Mg/Al ≤ 0.8. Increase in Mg/Al ratio leads to crystallize Mg(OH)<sub>2</sub>, which prevents successful morphological control in μm scale. Among the compositions, Mg/Al = 0.8 is expected to contain the largest LDH amount with channel formation allowed. The discussion below is focused on the results for the nominal molar ratio of Mg/Al = 0.8.



**Table 2.** Mg/Al ratios for the xerogel treated with NaOH solutions.

	Mg/Al (atomic ratio)
Xerogel	0.28
Xerogel treated with 0.1 M NaOH	0.91
Xerogel treated with 5 M NaOH	2.0
Xerogel treated with 10 M NaOH	2.0

**Figure 4.** (a and b) FE-SEM (c) TEM images of xerogel. The inset of (c) shows an electron diffraction pattern and the corresponding assignment. (d) Schematic illustration of agglomeration state of primary particles: green: LDH crystals; yellow: aluminum hydroxide.

phase separation is driven by entropy loss due to the growth of aluminate oligomers as pH increases.<sup>34</sup> The present Al-rich starting composition (Mg/Al=0.8) also brings about phase separation against the incorporated PEO additive. The evolution of phase separation can be tuned by the starting composition which regulates the compatibility between components. Here, we set the amount of PEO so that co-continuous phase-separated domains are quenched by sol-gel transition. As a result, phase separation accompanied by sol-gel transition forms interconnected two phases, *i.e.*, PEO-rich fluid phase and LDH/aluminate-rich solid phase.<sup>34, 36</sup> Subsequent evaporative drying step extracts the fluid phase to leave the macrochannel inside the xerogel. A magnified cross-sectional SEM image of the xerogel (Fig. 4b) shows mesochannel embedded in the gel skeletons. The mesochannel is formed as interstices of primary/secondary particles which can contribute to increase the surface area; BET surface area is 238 m<sup>2</sup>·g<sup>-1</sup> and the median mesopore size is 8.2 nm (See the sample denoted as c-gel-hierarchical in Table 3). The contribution of macrochannels to surface area is estimated < 10 m<sup>2</sup>·g<sup>-1</sup>,<sup>37</sup> indicating that the relatively high surface area of the hierarchical sample is due to the accessible mesoporosity. The primary particles have a plate-like morphology corresponding to two dimensional architectures of hydroxide crystals (Fig. 4c). The electron diffraction in the inset of Fig. 4c supports that the platelets are composed of LDH nanocrystals. The gel network is homogenous as clearly identified by SEM and TEM images. No trace of segregation

Representative photographs of LDH-based monolithic xerogel are shown in Fig. 2. The xerogel have a monolithic form with a cm-scale dimension. Fig. 3a shows a XRD pattern of the obtained xerogel. All the peaks can be ascribed to Mg-Al type hydrotalcite.<sup>26, 27</sup> The crystalline size estimated by the Scherrer's equation using from (003) diffraction line is 6.9 nm. The nanocrystalline nature is accounted for by high degree of supersaturation at the initial stage of the reaction. The hydroxide layer of the LDH is originated from brucite (Mg(OH)<sub>2</sub>) structure. When Mg<sup>2+</sup> cations are partially replaced with Al<sup>3+</sup> cations, electrical neutrality in a whole crystal is maintained by insertion of anions between hydroxide sheets. Hydrotalcite-type LDHs are typically synthesized in a basic solution (pH≈10),<sup>14</sup> where CO<sub>3</sub><sup>2-</sup> is incorporated because of its high affinity to hydroxide layers.<sup>28, 29</sup> On the other hand, the present condition (pH <4.0) avoids insertion of CO<sub>3</sub><sup>2-</sup> (See Supplementary Fig. S2), leading to selective introduction of Cl<sup>-</sup> in interlayers. Figure 3b shows a relationship between [OH<sup>-</sup>] and time since xerogel immersion in a NaOH solution (pH=10). The Cl<sup>-</sup> anions in interlayers are exchanged with OH<sup>-</sup> to gradually decrease [OH<sup>-</sup>] of the solution. Release of Cl<sup>-</sup> from interlayers was confirmed by adding AgNO<sub>3</sub> aqueous solution to the supernatant (inset of Fig. 3b). Fig. 3c shows TG-DTA curves of the xerogel. The first endothermic peak around at 100 °C corresponds to elimination of adsorbed water. The second endothermic region at temperature above 200 °C is derived from dehydroxylation of the layers and loss of Cl<sup>-</sup> anions.<sup>26, 27</sup> Relatively low crystallization temperature (445 °C) is a well-known feature of hydrotalcite-type LDHs;<sup>14</sup> LDHs have been a promising starting material for mixed metal oxides at a low temperature<sup>30</sup>. It should be pointed out that LDHs intercalated with Cl<sup>-</sup> can be used as a base material to design functional LDHs incorporating various organic/inorganic anions.<sup>31, 32</sup>

It has been reported that Mg/Al ratio of hydrotalcite-type LDH takes a value between 2 and 4.<sup>33</sup> The nominal Mg/Al ratio was set at 0.8 in the present study, which implies that excessive Al (III) ions form aluminum hydroxides. Indeed amorphous-like aluminum hydroxide forms in the preparation free from MgCl<sub>2</sub>·6H<sub>2</sub>O (See Supplementary Fig. S3). The compositions of LDH crystal and its relative ratio were estimated by selectively dissolving aluminum hydroxide contained in the xerogel. Table 2 summarizes Mg/Al ratios of the xerogel at respective experimental steps. LDH crystal comprising of the xerogel shows a Mg/Al value of 2.0, which means that the constituent LDH shows the highest charge-density among possible Mg-Al hydrotalcites (Mg/Al = 2-4). Based on the results of TG curve in Fig. 3c and Table 2, the composition of the xerogel has been calculated as [Mg<sub>0.66</sub>Al<sub>0.33</sub>(OH)<sub>2</sub>Cl<sub>0.33</sub>·2.92H<sub>2</sub>O]·3.1Al(OH)<sub>3</sub>. The aluminum hydroxide included in the xerogel works as a structural support, which is crucially important for morphological control as discussed below.

#### Spontaneous channel formation during sol-gel processing

Figure 4 shows SEM and TEM images of microstructures of the xerogel. Well-defined interconnected macrochannel with the diameter of ~1 μm (Fig. 4a) forms as a result of phase separation.<sup>23</sup> Phase separation has been demonstrated to occur between aluminate and PEO in the case that PO works as a proton scavenger in a solution of AlCl<sub>3</sub>·6H<sub>2</sub>O and PEO.<sup>34, 35</sup> Where,

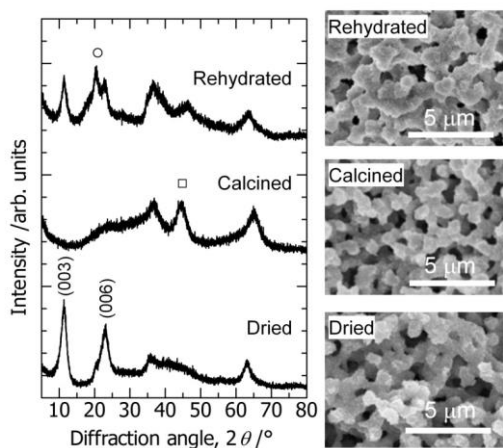


**Figure 5.** XRD patterns and SEM images of xerogel at respective steps in rehydration process with  $\text{Na}_2\text{CO}_3$  solution.  $\circ$ :  $\text{Al}(\text{OH})_3$  (Gibbsite);  $\square$ :  $\text{MgAl}_2\text{O}_4$ .

**Table 3.** Mesochannel characteristics of c-gels and c-pellet. The c-gel without macrochannel (c-gel-meso) was prepared without adding PEO in the step of xerogel synthesis.

	BET surface area ( $\text{m}^2\cdot\text{g}^{-1}$ )	Median Pore diameter (nm)	pore volume ( $\text{cm}^3\cdot\text{g}^{-1}$ )
c-gel-hierarchical	238	8.2	0.42
c-gel-meso	264	12.2	0.52
c-pellet	142	4.9	0.26

could be observed by SEM-EDX mapping and TEM diffraction pattern, indicating size of amorphous aluminate is also at nm scale and homogeneously-dispersed in the gel matrix. Homogeneously-distributed amorphous aluminum hydroxide works as a structural support (Fig. 4d); indeed, removal of aluminum hydroxide by using a basic solution results in collapse of the monolithic structure. Alternative routes to obtain LDH crystals are post-treatments applied to precursory oxides, such as a hot water treatment.<sup>38</sup> Decreasing crystal size and increasing number of nuclei are convincing requirements when oxides with macrochannel are used as a scaffold.<sup>37</sup> However, this requires troublesome tuning of supersaturation conditions. In this viewpoint, the spontaneous formation of channels composed of nanocrystalline LDHs has a considerable advantage. A brief summary of distinguished aspects of the obtained xerogel is as follows: (1) monolithic form; (2) interconnected hierarchical channels; (3) nanocomposite of aluminum hydroxide and high charge-density LDHs.

#### Processing of rehydration on monolithic xerogel with interconnected channels

As shown in the TG-DTA curve (Fig. 3c), anion species and water in the interlayers can be removed by the calcination at  $500^\circ\text{C}$ . By subsequently immersing the calcined gel into a solution of desired anions, those anions are reintroduced between hydroxide sheets (the process called as rehydration). Figure 5 shows XRD patterns and SEM images of gels at respective steps for rehydration. The calcination removes  $\text{Cl}^-$  and water molecules embedded in interlayers to lead to disappearance of (003) and

(006) diffractions of LDH crystals. The rehydration can recover the diffractions ascribed to (003) and (006), which suggests  $\text{CO}_3^{2-}$  ions are introduced into the interlayers to reform a layered structure. The introduction of  $\text{CO}_3^{2-}$  ions upon rehydration has been confirmed by FT-IR analysis (See Supplementary Fig. S4). It should be highlighted that morphologies of macrochannel are identical through the steps of calcination and rehydration. The feature would create advantages because relatively large anions can be introduced via rehydration with the macrochannel maintained.

#### Effect of channel formation on sorption property

The introduction of interconnected hierarchical channel can provide a potential means to monolithic LDHs with significant sorption characteristics. To confirm this possibility, sorption behaviors in pyranine solution were compared among the calcined xerogels (c-gels) and the calcined reference pellet (c-pellet). Table 3 summarizes channel characteristics of c-gels and c-pellet. We refer c-gel with only mesochannel as c-gel-meso and the c-gel with hierarchical channel as c-gel-hierarchical. The c-pellet shows the smallest BET specific surface, diameter of mesochannel, and mesopore volume among the samples. The mesochannel morphologies differ between c-gel-meso and c-gel-hierarchical because the occurrence of phase separation results in the pore diameter area and pore volume. Phase-separated primary particles should take a more packed and dense nanostructure compared to the case free from phase separation,<sup>35, 39</sup> resulting in the difference of mesochannel characteristics between c-gel-meso and c-gel-hierarchical.

Pyranine, which dissolves in water as a trivalent anion, was used as a fluorescent probe to investigate the effect of channels on sorption. The adsorbed pyranine on the samples was estimated by a change of UV-Vis spectra of supernatant liquid (Fig 6a). The sorption with the pyranine aqueous solution doesn't recover a prominent (003) peak of LDHs. Pyranine is therefore dominantly adsorbed on surface sites rather than intercalated in interlayers, though we can't completely deny trace amount of pyranine intercalated at layers' edges.<sup>40</sup> The adsorbed pyranine was released by subsequent anion exchange with  $\text{Na}_2\text{CO}_3$  aqueous solution (pH =10) (Inset images of Fig. 6a), indicating the possibility of entrapping/releasing ions with this material. Fig. 6b shows time-dependence of pyranine adsorption on the samples. The difference between c-pellet and c-gel-meso is primarily derived from the incorporation of larger mesochannels through which pyranine molecules can diffuse. The presence of the larger mesochannel facilitates gradual increase of  $n_{\text{pyranine}}$  for c-gel-meso ( $> 10$  h). The molecular diffusion through macrochannel leads to significant and rapid adsorption of pyranine on c-gel-hierarchical. The highest  $n_{\text{pyranine}}$  of c-gel-hierarchical is explained by the fact that the penetration of molecules inside the monolith allows the effective rehydration throughout the sample. The gradual saturation of  $n_{\text{pyranine}}$  ( $> 10$  h) can be accounted for by the rate-limiting slow diffusion in mesochannel. The contribution of mesochannel is also supported by Supplementary Fig. S5. Significant increase of  $n_{\text{pyranine}}$  is observed for c-powder compared to c-pellet, however,  $n_{\text{pyranine}}$  shows a plateau at 10 h and no gradual increase is observed for c-powder.

Another point should be mentioned is difference of crystalline nature among the samples. Fig. 6c shows Langmuir plots for c-

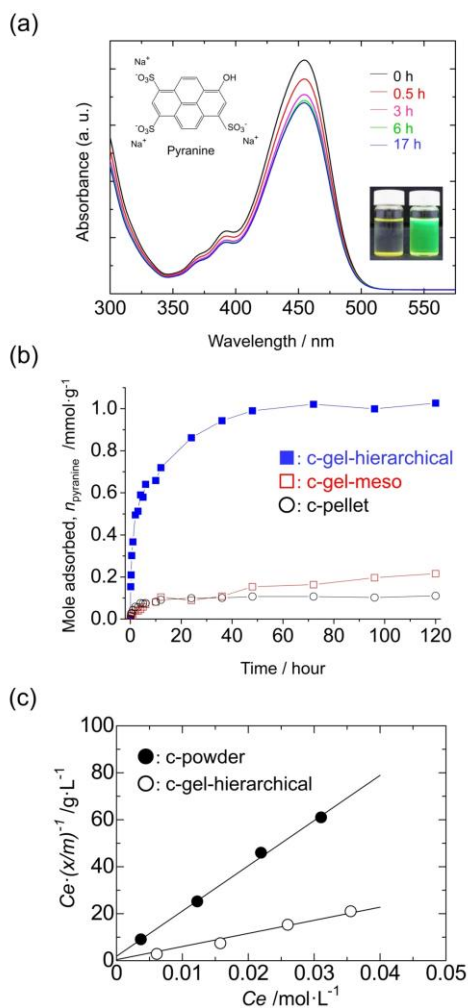


**Figure 6.** (a) Time variation of UV-Vis spectra of the pyranine aqueous solution containing c-gel-hierarchical as an adsorbent. Inset images: the pyranine-adsorbed gel was immersed in (left image) water and (right image)  $\text{Na}_2\text{CO}_3$  solution (pH = 10). (b) Time dependence of pyranine adsorption: ■: c-gel-hierarchical; □: c-gel-meso; ○: c-pellet.  $n_{\text{pyranine}}$ : mole of pyranine adsorbed per unit mass of adsorbate. (c) Langmuir plots of c-powder (●) and c-gel-hierarchical (○).

powder and c-gel-hierarchical, where  $C_e$  is the equilibrium concentration of pyranine in the solution ( $\text{mol} \cdot \text{L}^{-1}$ ),  $x/m$  denotes the amount of adsorbed pyranine per unit mass of constituent LDHs ( $\text{mol} \cdot \text{g}^{-1}$ ).<sup>41–43</sup> From the linear fitting on Fig. 6c, adsorption capacity per unit mass of LDH crystals are estimated as  $5.2 \times 10^{-4} \text{ mol} \cdot \text{g}^{-1}$  and  $1.8 \times 10^{-3} \text{ mol} \cdot \text{g}^{-1}$  for c-powder and c-gel-hierarchical, respectively. The high capacity of c-gel-hierarchical is derived from the high charge density of hydroxide layers ( $\text{Mg}/\text{Al} = 2.0$ )<sup>44</sup> and the small size of LDH crystallites (See Supplementary Fig. S6). The small LDH crystallites certainly contribute to the increase of adsorption capacity and adsorption rate because abundant adsorption sites are accessible by pyranine molecules. It can be concluded that the better adsorption characteristics of c-gel-hierarchical are originated from the successful channel formation and the characteristic crystalline nature of LDH comprising xerogels.

## Conclusions

LDH-based monoliths with accessible hierarchical channels have been fabricated via an epoxide-mediated sol-gel reaction. Xerogels are obtained as a composite comprised of aluminum hydroxide and Mg–Al–Cl hydrotalcite-type LDH. LDH comprising xerogels shows nanocrystalline nature with a crystallite size of 6.9 nm and a BET surface of  $238 \text{ m}^2 \cdot \text{g}^{-1}$ . Homogeneously-dispersed aluminum hydroxide crystals work as a structural support, which facilitate the spontaneous channel formation. The xerogels possess interconnected hierarchical channels in  $\mu\text{m}$  and nm ranges with the size of 1.0  $\mu\text{m}$  and 8.2 nm, respectively. The channel structures are maintained in the course of rehydration processing, affording the formation of monolithic LDH intercalated with relatively large anion species. Sorption test with an aqueous pyranine solution revealed that macrochannels considerably enhance sorption affinity. Slow diffusion of anion species in the mesochannels and high charge density of obtained LDH also contribute the enhanced adsorption capability. As a result, considerable accumulation of anionic species as well as drastically-improved adsorption rate have been demonstrated in monolithic LDHs with a cm-scale. The simple procedure presented here can be applied to wide variety of LDH systems, which opens up applications of monolithic LDHs free from diffusion limitation.

## Acknowledgements

The present work is partially supported by Grant-in-Aid for Scientific Research (B) (No. 22360276), and Grant-in-Aid for Young Scientists (B) (No. 24750206) from the Ministry of Education, Culture, Sports, Science and Technology (MEXT), administrated by Japan Society for the Promotion of Science (JSPS). Y. T. is also partially supported financially by a research grant from The Murata Scientific Foundation.

## Notes and references

- <sup>a</sup> Department of Materials Science, Graduate School of Engineering, Osaka Prefecture University, Sakai, Osaka, 599-8531, Japan.
- <sup>b</sup> Department of Chemistry, Graduate School of Science, Kyoto University, Kitashirakawa, Sakyo-ku, Kyoto, 606-8502, Japan.
- \* To whom correspondence should be addressed: E-mail: tokudome@photomater.com Tel/Fax: +81-72-254-7598/+81-72-254-7598 (Y. Tokudome)
- † Electronic Supplementary Information (ESI) available: [FT-IR spectra, XRD patterns, a pH-time curve, results of pyranine adsorption experiments.]. See DOI: 10.1039/b000000x/
1. M. Ogawa and K. Kuroda, *Bull. Chem. Soc. Jpn.*, 1997, **70**, 2593–2618.
2. P. Umek, P. Cevc, A. Jesih, A. Gloter, C. P. Ewels and D. Arcon, *Chem. Mater.*, 2005, **17**, 5945–5950.
3. F. Millange, R. I. Walton, L. X. Lei and D. O'Hare, *Chem. Mater.*, 2000, **12**, 1990–1994.
4. B. M. Choudary, S. Madhi, N. S. Chowdari, M. L. Kantam and B. Sreedhar, *J. Am. Chem. Soc.*, 2002, **124**, 14127–14136.
5. L. A. Vermeulen and M. E. Thompson, *Nature*, 1992, **358**, 656–658.
6. Q. Wang and D. O'Hare, *Chem. Rev.*, 2012, **112**, 4124–4155.
7. G. R. Williams and D. O'Hare, *J. Mater. Chem.*, 2006, **16**, 3065–3074.
8. B. V. Lotsch and G. A. Ozin, *Adv. Mater.*, 2008, **20**, 4079–4084.

9. B. N. Pal, B. M. Dhar, K. C. See and H. E. Katz, *Nat Mater*, 2009, **8**, 898-903.
10. K. Hosono, I. Matsubara, N. Murayama, S. Woosuck and N. Izu, *Chem. Mater.*, 2005, **17**, 349-354.
- 5 11. D. G. Cantrell, L. J. Gillie, A. F. Lee and K. Wilson, *Appl Catal a-Gen*, 2005, **287**, 183-190.
12. F. Cavani, F. Trifiro and A. Vaccari, *Catal. Today*, 1991, **11**, 173-301.
13. V. Rives, *Nova Science Publishers, Inc: New York*, 2001.
14. V. R. L. Constantino and T. J. Pinnavaia, *Inorg. Chem.*, 1995, **34**, 883-892.
- 10 15. G. W. Brindley and S. Kikkawa, *Am. Mineral.*, 1979, **64**, 836-843.
16. A. B. Bourlinos, D. D. Jiang and E. P. Giannelis, *Chem. Mater.*, 2004, **16**, 2404-2410.
17. P. A. Wheeler, J. Z. Wang and L. J. Mathias, *Chem. Mater.*, 2006, **18**, 3937-3945.
- 15 18. Y. S. Tao, H. Kanoh, L. Abrams and K. Kaneko, *Chem. Rev.*, 2006, **106**, 896-910.
19. Y. J. Lee, J. S. Lee, Y. S. Park and K. B. Yoon, *Adv. Mater.*, 2001, **13**, 1259-1263.
- 20 20. B. T. Holland, C. F. Blanford and A. Stein, *Science*, 1998, **281**, 538-540.
21. J. E. G. J. Wijnhoven and W. L. Vos, *Science*, 1998, **281**, 802-804.
22. S. S. Kim, J. Shah and T. J. Pinnavaia, *Chem. Mater.*, 2003, **15**, 1664-1668.
- 23 23. K. Nakanishi, *J. Porous Mater.*, 1997, **4**, 67-112.
24. A. E. Gash, T. M. Tillotson, J. H. Satcher, J. F. Poco, L. W. Hrubesh and R. L. Simpson, *Chem. Mater.*, 2001, **13**, 999-1007.
25. A. E. Gash, T. M. Tillotson, J. H. Satcher, L. W. Hrubesh and R. L. Simpson, *J. Non-Cryst. Solids*, 2001, **285**, 22-28.
- 30 26. R. Chitrakar, S. Tezuka, A. Sonoda, K. Sakane and T. Hirotsu, *Industrial & Engineering Chemistry Research*, 2008, **47**, 4905-4908.
27. F. Prinetto, G. Ghiotti, P. Graffin and D. Tichit, *Microporous Mesoporous Mater.*, 2000, **39**, 229-247.
- 35 28. Z. P. Liu, R. Z. Ma, M. Osada, N. Iyi, Y. Ebina, K. Takada and T. Sasaki, *J. Am. Chem. Soc.*, 2006, **128**, 4872-4880.
29. N. Iyi, T. Matsumoto, Y. Kaneko and K. Kitamura, *Chem. Mater.*, 2004, **16**, 2926-2932.
30. A. Kudo, K. Omori and H. Kato, *J. Am. Chem. Soc.*, 1999, **121**, 11459-11467.
- 40 31. M. Meyn, K. Beneke and G. Lagaly, *Inorg. Chem.*, 1990, **29**, 5201-5207.
32. S. Miyata, *Clays Clay Miner.*, 1983, **31**, 305-311.
33. U. Costantino, F. Marmottini, M. Nocchetti and R. Vivani, *Eur. J. Inorg. Chem.*, 1998, 1439-1446.
- 45 34. Y. Tokudome, K. Fujita, K. Nakanishi, K. Miura and K. Hirao, *Chem. Mater.*, 2007, **19**, 3393-3398.
35. Y. Tokudome, K. Nakanishi, K. Kanamori and T. Hanada, *J. Colloid Interface Sci.*, 2010, **352**, 303-308.
- 50 36. K. Nakanishi and N. Tanaka, *Acc. Chem. Res.*, 2007, **40**, 863-873.
37. Y. Tokudome, K. Nakanishi, S. Kosaka, A. Kariya, H. Kaji and T. Hanada, *Microporous Mesoporous Mater.*, 2010, **132**, 538-542.
38. N. Yamaguchi, T. Nakamura, K. Tadanaga, A. Matsuda, T. Minami and M. Tatsumisago, *Chem. Lett.*, 2006, **35**, 174-175.
- 55 39. K. Kanamori, Y. Kadera, G. Hayase, K. Nakanishi and T. Hanada, *J. Colloid Interface Sci.*, 2011, **357**, 336-344.
40. E. Geraud, M. Bouhent, Z. Derriche, F. Leroux, V. Prevot and C. Forano, *J. Phys. Chem. Solids*, 2007, **68**, 818-823.
41. J. Das, B. S. Patra, N. Baliarsingh and K. M. Parida, *Appl Clay Sci*, 2006, **32**, 252-260.
- 60 42. Y. W. You, H. T. Zhao and G. F. Vance, *Colloids and Surfaces a-Physicochemical and Engineering Aspects*, 2002, **205**, 161-172.
43. Y. You, G. F. Vance and H. Zhao, *Appl Clay Sci*, 2001, **20**, 13-25.
- 65 44. T. Hibino and A. Tsunashima, *Chem. Mater.*, 1998, **10**, 4055-4061.